PCCP

PAPER

View Article Online
View Journal | View Issue



Cite this: *Phys. Chem. Chem. Phys.*, 2017, **19**, 7188

# Decay times of the spin-forbidden and spin-enabled transitions of $Yb^{2+}$ doped in $CsCaX_3$ and $CsSrX_3$ (X = Cl, Br, I)

Markus Suta,[a] Tim Senden,[b] Jacob Olchowka,[a] Matthias Adlung,[a] Andries Meijerink*[b] and Claudia Wickleder*[a]

Received 26th January 2017,
Accepted 13th February 2017

DOI: 10.1039/c7cp00581d

rsc.li/pccp

In this paper, a systematic study of the decay times of the spin-enabled and spin-forbidden transitions of $Yb^{2+}$ doped into the halidoperovskites $CsMX_3$ (M = Ca, Sr; X = Cl, Br, I) is presented. The spin-forbidden transitions are characterized by ms decay times, which are typical for $Yb^{2+}$. On the contrary, the spin-enabled transitions show much shorter decay times in the range of μs and have so far only been rarely observed. These results allow detailed conclusions about systematics of the decay times of $Yb^{2+}$ doped in similar compounds and their correlation to the local structure of the coordination sphere of $Yb^{2+}$ as well as the role of vibrational interaction between the excited high spin (HS) and low spin (LS) states. The halidoperovskites are ideally suited as host lattices in this context and may work as text book examples due to their comparable structures, which allows a detailed interpretation of the decay times in relation to the local structure. An understanding of the impact of the composition and structure of the host material on the decay times of $Yb^{2+}$ will be of relevance for future applications of this activator in scintillators or lighting materials.



## 1 Introduction

Divalent lanthanides have gained considerable interest in the last few decades due to their electric-dipole allowed $4f^{n-1}5d \rightarrow 4f^n$ transitions that are typically located in the UV and visible range. $Eu^{2+}$ is by far the most investigated ion because of its applications in bulk as well as nanostructured materials and its chemical stability in many solids combined with the tunability of the emission colour over the full visible range.[1,2] A similar behaviour is found for $Yb^{2+}$ with a full-shell $4f^{14}$ configuration in its electronic ground state, although this ion is much less investigated due to the more difficult preparation and lower chemical stability in the divalent state. Unlike $Eu^{2+}$, $Yb^{2+}$ has no excited 4f states located in the near UV range and hence only shows broad-band 4f–5d transitions even if the lowest 5d state is positioned at relatively high energy. Moreover, due to the presence of both excited triplet and singlet states, which are often termed as high spin (HS) and low spin (LS) states, in general two emission bands can be observed.[3] However, theoretical works also indicated that spin–orbit coupling is non-negligible for $Yb^{2+}$, which makes a spin assignment for the excited states somewhat questionable.[4–6] Due to this effect, it was pointed out that the term spin-enabled instead of spin-allowed is more suitable in relation to previous theoretical studies in $Yb^{2+}$-activated $SrCl_2$ and $CsCaBr_3$ in which it was shown that even the first excited LS state shows a considerable admixture with triplet states, thus making a spin designation actually not very reliable.[4–6]

Many investigations on the luminescence of $Yb^{2+}$ have been conducted on alkali halides[7–9] and $SrCl_2$[4,5,10] with local cubic symmetries at the cation sites, but also other $Yb^{2+}$-activated compounds with lower site symmetries such as borates,[11,12] phosphates,[13] sulfates,[14] sulfides[15] or nitridosilicates[16,17] have already been in the focus of research. Besides experimental investigations, the small number of microstates of the excited $4f^{13}5d$ configuration allows for theoretical approaches, most of which are semi-empirical in nature.[5,9,18] For the particular cases of $Yb^{2+}$-activated $SrCl_2$ and $CsCaBr_3$, which provide highly symmetric cation sites, *ab initio* approaches were also attempted that allow for a theoretical prediction of decay times of the excited states as well.[6,19,20–22] Another promising approach combines ligand field theory with DFT calculations, which has been reported to provide very reliable predictions of the optical properties of divalent lanthanides, even in the case of the theoretically more demanding $Eu^{2+}$ ions.[23,24]

Recently, we have reported on the luminescence properties of $Yb^{2+}$ doped into the halidoperovskites $CsMX_3$ (M = Ca, Sr; X = Cl, Br, I) that provide highly symmetric sites for the divalent

[a] *Inorganic Chemistry, Faculty of Science and Technology, University of Siegen, Adolf-Reichwein-Str. 2, 57068 Siegen, Germany. E-mail: wickleder@chemie.uni-siegen.de*
[b] *Condensed Matter and Interfaces, Debye Institute for Nanomaterials Science, Utrecht University, Princetonplein 5, P.O. Box 80 000, 3584 CC Utrecht, The Netherlands. E-mail: a.meijerink@uu.nl*

lanthanide ion and therefore give rise to very well-resolved luminescence spectra with a rich fine structure at low temperatures.[25] Moreover, it has been shown that the excited HS state of $Yb^{2+}$ can be populated upon excitation into the LS state by a thermally assisted vibrational relaxation.[5,8] The temperatures required for efficient population of the HS states and thus for an intense spin-forbidden emission are very much dependent on the vibrational energies of the local modes of the coordination polyhedron surrounding the $Yb^{2+}$ ions.[26] This mechanism, however, also leads to a vibrationally assisted mixing of the HS and LS states, which has an impact on the observable decay times for both the spin-forbidden and spin-allowed emission.[8] Due to the fact that the spin-forbidden $4f^{14} \leftrightarrow 4f^{13}5d^1$ transition of $Yb^{2+}$ in cubic symmetries is also symmetry-forbidden, whereas the spin-allowed one is also symmetry-allowed, the decay times of both transitions provide valuable information about the local structure and vibrational interaction dependent on the temperature.[8]

Numerous decay times have been reported for the spin- and symmetry-forbidden transitions of $Yb^{2+}$ in a wide variety of host compounds such as sulfates,[14] $SrB_4O_7$,[11] phosphates,[13] fluorides such as $MF_2$ (M = Mg–Ba)[27,28] or $AMgF_3$ (A = Na, K)[29] and fluoridohalides MFX (M = Ca, Sr; X = Cl, Br).[30] They typically lie in the range of tens of milliseconds and are particularly long below 10 K for highly ionic hosts that exhibit high vibrational energies. On the contrary, decay times of the spin-allowed transition of $Yb^{2+}$ are only scarcely reported in the literature due to its rare observation and are limited to few examples such as $SrCl_2$:$Yb^{2+}$,[5] NaCl:$Yb^{2+}$ [8] or $SrI_2$:$Yb^{2+}$.[31] They are characterized by values in the range of several microseconds, even at low temperatures down to 20 K. However, to the best of our knowledge, no clear correlation studies between the values of the decay times of both $Yb^{2+}$-based transitions and the local structure of the coordination sphere as well as factors like varying vibrational interaction and covalence have been reported up to now.

For that reason, we here present such a systematic investigation of the $Yb^{2+}$-activated halidoperovskites $CsCaX_3$ and $CsSrX_3$ (X = Cl, Br, I). These materials provide an excellent model system for this study as not only high-symmetry cation sites in several hosts with comparable coordination spheres, but also the effect of bond lengths and subtle symmetry distortions such as in $CsSrI_3$ are given.[32] Moreover, knowledge about the variation of the decay times of $Yb^{2+}$ in these compounds may allow drawing conclusions for other compounds to gain a better insight into the optical properties of this divalent ion. This might be of relevance for the design of novel luminescent materials based on $Yb^{2+}$ luminescence, as has already been pointed out in the field of scintillators.[26,33]

## 2 Experimental

The synthesis of the $Yb^{2+}$-doped halidoperovskites $CsMX_3$ (M = Ca, Sr; X = Cl, Br, I) (doping concentration of 0.1 mol%) has already been reported by us in a previous publication.[25] For the measurements of the decay times of $Yb^{2+}$, only clear and transparent pieces of the samples ($\sim$1 $mm^3$) were used and sealed in thin evacuated quartz ampoules due to its air and moisture sensitivity. The decay times of the spin-forbidden transition were measured at both 10 K and 300 K using a Xe flash lamp (75 W) attached on a Fluorolog-3 FL3-22 spectrometer (Horiba Jobin Yvon) as an excitation source. The emission was detected by using a photon counting system (R928P, Hamamatsu). The samples were cooled down to 10 K in a He closed-cycle cryostat (Janis) and an external temperature control unit (Lake Shore). The decay times of the spin-allowed transitions were measured on an FL3920 fluorescence spectrometer (Edinburgh Instruments). Excitation was performed using a pulsed diode laser (Edinburgh EPL375, $\lambda_{ex}$ = 376.8 nm) with a pulse width of 65 ps and a variable repetition rate in the range of 20 kHz to 20 MHz. The decay curves were recorded using a photomultiplier tube (Hamamatsu H7422-40) in combination with time-correlated single-photon counting (TCSPC) on a TCC900 computer card (Edinburgh). For measurements down to 4 K, the samples were cooled down in a liquid He flow cryostat (Oxford Instruments).

## 3 Results and discussion

### 3.1 Spin-forbidden $4f^{13}5d^1 \rightarrow 4f^{14}$ transitions of $Yb^{2+}$

The photoluminescence of $Yb^{2+}$ doped into the halides $CsMX_3$ (M = Ca, Sr; X = Cl, Br, I) and its relation to the local site symmetries have already been described by us in detail in another publication.[25] The effect of $Yb^{3+}$ impurities formed during synthesis was also verified and only a very weak ($CsSrCl_3$) or even no $4f^{13} \rightarrow 4f^{13}$ luminescence could be found in the presented halides implying the high stability of $Yb^{2+}$ in these hosts. Together with the low concentration of 0.1 mol%, we can conclude that no additional symmetry distortion should be expected due to charge-compensating defects based on $Yb^{3+}$.

In all hosts, $Yb^{2+}$ shows two emissions in the violet to blue range, out of which the lower energetic one is assigned to the spin-forbidden $4f^{13}5d^1$(HS) $\rightarrow 4f^{14}$ transition. The luminescence decay curves obtained upon selective excitation into the $4f^{13}(^2F_{7/2})5d^1(t_{2g}$, HS) state are depicted in Fig. 1. Almost all decay curves can be fitted to a single exponential decay, both at 10 K and 300 K. The corresponding decay times are summarized in Table 1. All decay times lie in the ms range, which justifies the assignment of the lower energetic emissions of $Yb^{2+}$ to a spin-forbidden transition. It is evident that the decay times for the corresponding transition of $Yb^{2+}$ in the Sr-based halides are all shorter than those in the respective Ca-based halides both at 10 K and room temperature (see Table 1). This may be related to the effect of symmetry. In a perfect octahedral environment, coupling of the $4f^{13}$ core to the $5d^1$ electron under inclusion of spin–orbit coupling leads to a transformation of the lowest HS states as $^{(3)}T_{2u}$ + $^{(3)}E_u$.[4,8] In $O_h$ symmetry, transitions from these states to the ground state $^{(1)}A_{1g}$ ($^1S_0$) are symmetry-forbidden and thus, the decay time of the excited HS states is particularly long. It should be noted that we put the spin designation in brackets as it actually loses its meaning within the framework of spin–orbit coupling.[5] From a spectroscopic point of view,

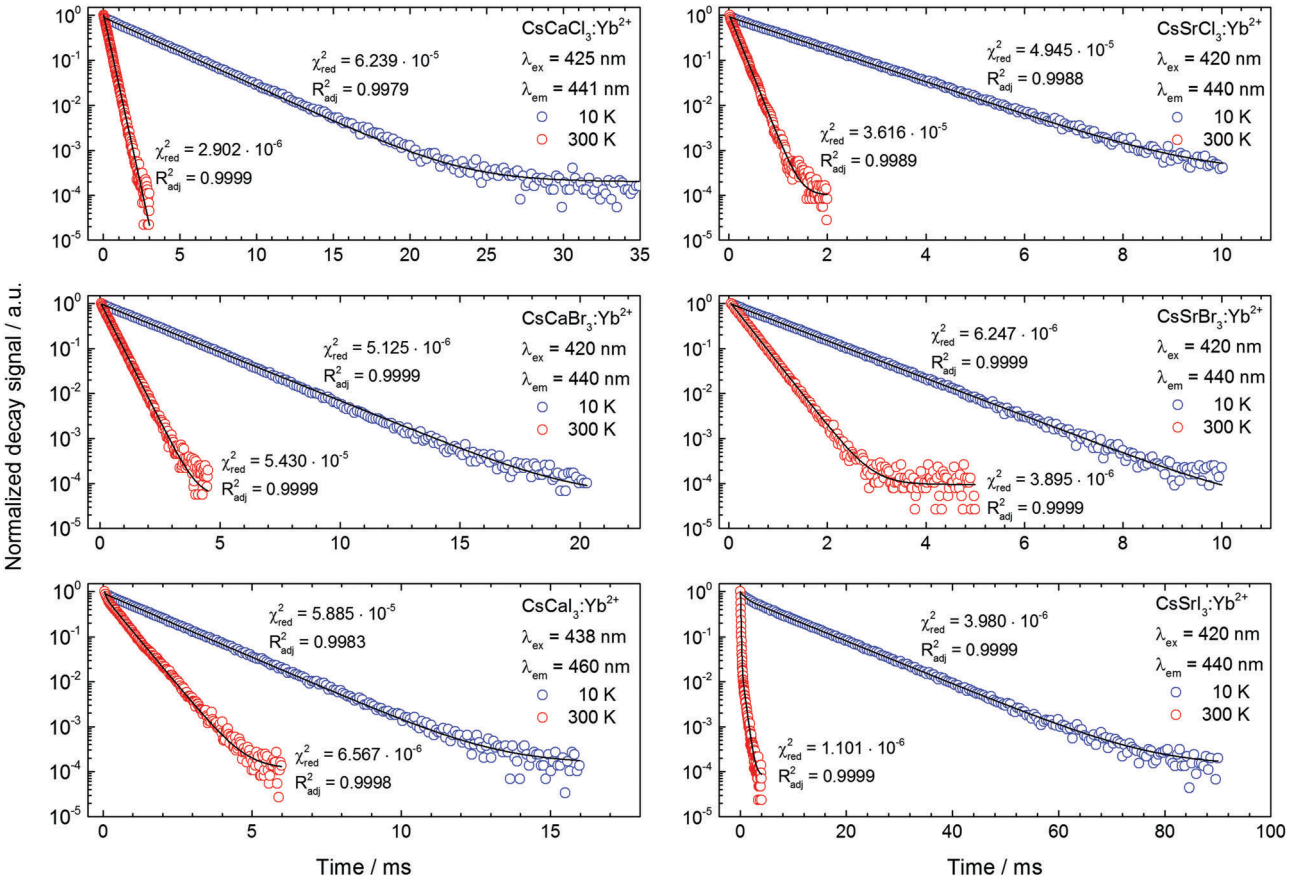


Fig. 1 Semi-logarithmic plots of the luminescence decay of the spin-forbidden transition $4f^{13}(^2F_{7/2})5d^1(HS) \rightarrow 4f^{14}(^1S_0)$ of $Yb^{2+}$ doped in $CsCaX_3$ and $CsSrX_3$ (X = Cl, Br, I) at 10 K (blue points) and 300 K (red points). Excitation and detected emission wavelengths are given in the graphs. Black lines indicate least-squares fits to single exponential decays or biexponential decays in the case of $CsSrI_3:Yb^{2+}$. Statistical figures of merit are given in each case and for the fitting results, see Table 1.

Table 1 Decay times of the excited HS state of $Yb^{2+}$ in $CsCaX_3$ and $CsSrX_3$ (X = Cl, Br, I) at 10 K and room temperature. Excitation and emission wavelengths are denoted in Fig. 1. Errors of the decay times are in the range of $10^{-3}$ ms and hence, disregarded here

| | $\tau_{HS}$/ms | |
|---|---|---|
| Compound | 10 K | 300 K |
| $CsCaCl_3:Yb^{2+}$ | 2.8 | 0.28 |
| $CsSrCl_3:Yb^{2+}$ | 1.19 | 0.16 |
| $CsCaBr_3:Yb^{2+}$ | 2 | 0.39 |
| $CsSrBr_3:Yb^{2+}$ | 1.04 | 0.31 |
| $CsCaI_3:Yb^{2+}$ | 1.53 | 0.54 |
| $CsSrI_3:Yb^{2+}$* | 0.87 | 0.07 |
| | 9.08 | 0.48 |

however, the differentiation between HS and LS states highly simplifies the discussion so we keep this designation, although it is only a first-order approximation and especially for the higher excited states, there is a strong mixing of singlet and triplet states.

Due to the similarity in the ionic radii of $Ca^{2+}$ and $Yb^{2+}$ ($r(Ca^{2+})$ = 1.00 Å, $r(Yb^{2+})$ = 1.01 Å for CN = 6),[34] the effect of distortion of the $Ca^{2+}$ sites upon substitution with $Yb^{2+}$ ions is negligible, whereas a more severe symmetry reduction is expected upon doping of the compounds $CsSrX_3$ (X = Cl, Br, I) due to the larger ionic radius of the $Sr^{2+}$ ions ($r(Sr^{2+})$ = 1.18 Å for CN = 6).[34] This slightly lifts the forbidden character of the transitions from the HS state in terms of symmetry and hence reduces the decay times in general. $CsSrI_3:Yb^{2+}$ is a special case in this series and hence, the extraordinarily long decay time at 10 K will be discussed separately below.

**3.1.1 Low temperature decay times.** At 10 K, vibrational relaxation is hindered to a large extent and the data allow drawing a clear correlation of the decay times to the local structure of the coordination sphere of $Yb^{2+}$ embedded in the presented halide hosts. Besides $CsSrI_3:Yb^{2+}$, which is excluded from the discussion due its special behaviour, in particular $CsCaCl_3:Yb^{2+}$ exhibits an extraordinarily long decay time for the spin-forbidden transition among the presented halides at low temperatures. The decay time then decreases for $Yb^{2+}$-activated $CsCaBr_3$ and further in the case of $CsCaI_3$ at 10 K. Similarly, a decrease in the 10 K decay times of the spin-forbidden transition is found from $CsSrCl_3:Yb^{2+}$ to $CsSrBr_3:Yb^{2+}$. This trend is related to the increasing covalence of the Yb–anion bond from Cl to I due to the fact that softer anions allow a higher change in the Yb–ligand distance of the excited state relative to the ground state. This leads to a larger rate of non-radiative relaxation into the ground state even at 10 K or,

 

within the frame of the configurational coordinate model, to a low lying crossing point between the potential of the excited HS state and the ground state. In fact, these results fit nicely to the variation of the Stokes shifts and Huang–Rhys parameters that we have reported earlier for $Yb^{2+}$ in these host compounds.[25,26] In general, there seems to be an inverse correlation of the decay times to the Yb–ligand bond length. This becomes particularly clear upon comparison of $CsCaBr_3$ with NaCl due to the similar average metal–ligand distances in both compounds.[35,36] Accordingly, the decay time of the spin-forbidden transition in $CsCaBr_3$:$Yb^{2+}$ is very similar to the one found for NaCl:$Yb^{2+}$ ($\tau$ = 1.4 ms at 20 K).[8] Moreover, the generally shorter decay times in $CsSrCl_3$:$Yb^{2+}$ and $CsSrBr_3$:$Yb^{2+}$ are consistent with the longer Yb–ligand distances compared to the Ca analogues and also fit into this correlation. Accordingly, the reported values of the decay times of spin-forbidden transitions of $Yb^{2+}$ in fluorides at low temperatures nicely agree with this trend as they are always particularly long ($\geq$7 ms) at temperatures in the range of 10 K and show a highly temperature-dependent non-radiative rate similar to $CsCaCl_3$:$Yb^{2+}$.[27–30]

$CsSrI_3$:$Yb^{2+}$ has already been shown to be a special case in this series due to a trigonal distortion at the $Sr^{2+}$ sites.[25] This is also reflected in the extraordinarily long decay time component of around 9 ms (see Table 1) at 10 K. This indicates a higher degree of symmetry forbidden character of this transition compared to the ones of the other compounds in this series. In this case, the local $D_{3d}$ symmetry causes the HS state to split into $^{(3)}T_{2u}$, $^{(3)}E_u$ and $^{(3)}A_{1u}$ components. According to the symmetry selection rules, only transitions from $^{(3)}E_u$ states to the ground state $^{(1)}A_{1g}$ are symmetry allowed. The long decay time component therefore highly suggests that the $^{(3)}A_{1u}$ state is located lowest in energy. This is in agreement with considerations from the angular overlap model (AOM) that lead to the same energetic order of the crystal field levels.[32] The observation of a second and faster decay component of 0.87 ms at 10 K (see Table 1) implies population of the higher excited $^{(3)}E_u$ state even at low temperatures and, because of slow non-radiative relaxation to the $^{(3)}A_{1u}$ state the radiative $^{(3)}E_u$–$^{(1)}A_{1g}$ decay gives rise to this second component. The symmetry-allowed character of this particular transition gives rise to the shortest decay time among all considered $Yb^{2+}$-doped halidoperovskites.

**3.1.2 Room temperature decay times.** At 300 K, the decay times generally decrease by around one order of magnitude compared to those at 10 K. The present results also show a shortening of the decay time of the high spin emission (see Table 1). When the room temperature decay times for the different halides are considered, we observed that the trend in the variation of the decay times of the spin-forbidden transition of $Yb^{2+}$ shows a behaviour opposite to the data obtained at 10 K, *i.e.* the decay times increase in magnitude for the heavier halides. Such a behaviour can be well related to the weaker vibrational interaction due to the lower effective vibrational energy of the $[YbX_6]^{4-}$ octahedra for the heavier halides that makes thermally activated non-radiative processes less efficient.[26] The lengthening of the room temperature decay times from the chloride over the bromide to the iodide may also be related to more effective mixing of the HS state with the LS states at room temperature induced by the higher energetic vibrational modes present in a chloride compared to the heavier halides. In fact, this mechanism was discussed as a possible reason for the observation of a spin- and symmetry-forbidden transition in cubic symmetries at all.[8,26]

The variation of the decay times in $CsSrI_3$:$Yb^{2+}$ highly confirms the model of trigonal distortion at the $Sr^{2+}$ sites. The short component of 0.07 ms (see Table 1) is assigned to the symmetry-allowed decay from the excited $^{(3)}E_u$ state. Interestingly, the long decay time component in $CsSrI_3$:$Yb^{2+}$ is highly reduced to 0.48 ms at room temperature. Based on our model, this is reasonable since non-radiative transitions from the $^{(3)}A_{1u}$ to both the excited $^{(3)}E_u$ and the ground state $^{(1)}A_{1g}$ occur. The non-radiative relaxation to the ground state is also enhanced by the induced splitting of the excited HS state in $D_{3d}$ symmetry that effectively decreases the energy gap to the ground state. The previous analysis confirms that $CsSrI_3$:$Yb^{2+}$ has to be regarded as a separate case compared to the other $Yb^{2+}$-activated halides discussed.

### 3.2 Spin-enabled $4f^{13}5d^1 \rightarrow 4f^{14}$ transitions of $Yb^{2+}$

The spin-enabled $4f^{13}5d^1 \rightarrow 4f^{14}$ emissions of $Yb^{2+}$ in the presented halides lie at slightly higher energies than the corresponding spin-forbidden emissions[25] and are characterized by shorter decay times that are typically in the range of a few µs.[5,8,31] It is noteworthy that there are only very few examples of reported decay times for this transition of $Yb^{2+}$ doped in inorganic solids, *e.g.* for $SrCl_2$:$Yb^{2+}$ (1.04 µs at 10 K; 0.55 µs at 300 K),[5] NaCl:$Yb^{2+}$ (2.68 µs at 20 K; 0.59 µs at 303 K)[8] or $SrI_2$:$Yb^{2+}$ (0.40 µs at 78 K).[31] Therefore, for the best of our knowledge, we present here the first systematic study on these decay times in this paper. For the spin-enabled transitions, single exponential decays are also observed at both 10 K and room temperature in almost all of the presented halidoperovskites (see Fig. 2) except for $CsSrI_3$:$Yb^{2+}$. The measured decay times are in similar ranges to the reported values mentioned above (see Table 2).[5,8,31] The decay times of the spin-enabled transitions of $Yb^{2+}$ in Sr-based halides are lower than those of the respective Ca-based analogues, in agreement with the results for the spin-forbidden transition (see Table 1). This is another manifestation of the higher symmetry distortion that occurs upon doping of the $Sr^{2+}$ sites with the smaller $Yb^{2+}$ ions.[34]

**3.2.1 Low temperature decay times.** The decay curves of the spin-enabled $4f^{13}5d^1 \rightarrow 4f^{14}$ transitions of $Yb^{2+}$ at 10 K are depicted in Fig. 2 (blue points) and were obtained upon laser excitation at 375 nm. Most of the $Yb^{2+}$-doped samples show single exponential decay curves at 10 K with decay times in the expected range of µs (see Table 2). The only exception is again $CsSrI_3$:$Yb^{2+}$, which will be discussed separately below. Unlike the decay times of the corresponding spin-forbidden transitions, the decay times of the spin-enabled $4f^{13}5d^1 \rightarrow 4f^{14}$ transitions do not show a clear regularity that allows drawing conclusions about changes in the $Yb^{2+}$–ligand distance of the excited states relative to the ground states. This becomes particularly obvious from the opposite trends in the decay times with varying halide anions for the Ca- and Sr-based chlorides and bromides (see Table 2). Self-absorption effects may be neglected as a possible reason

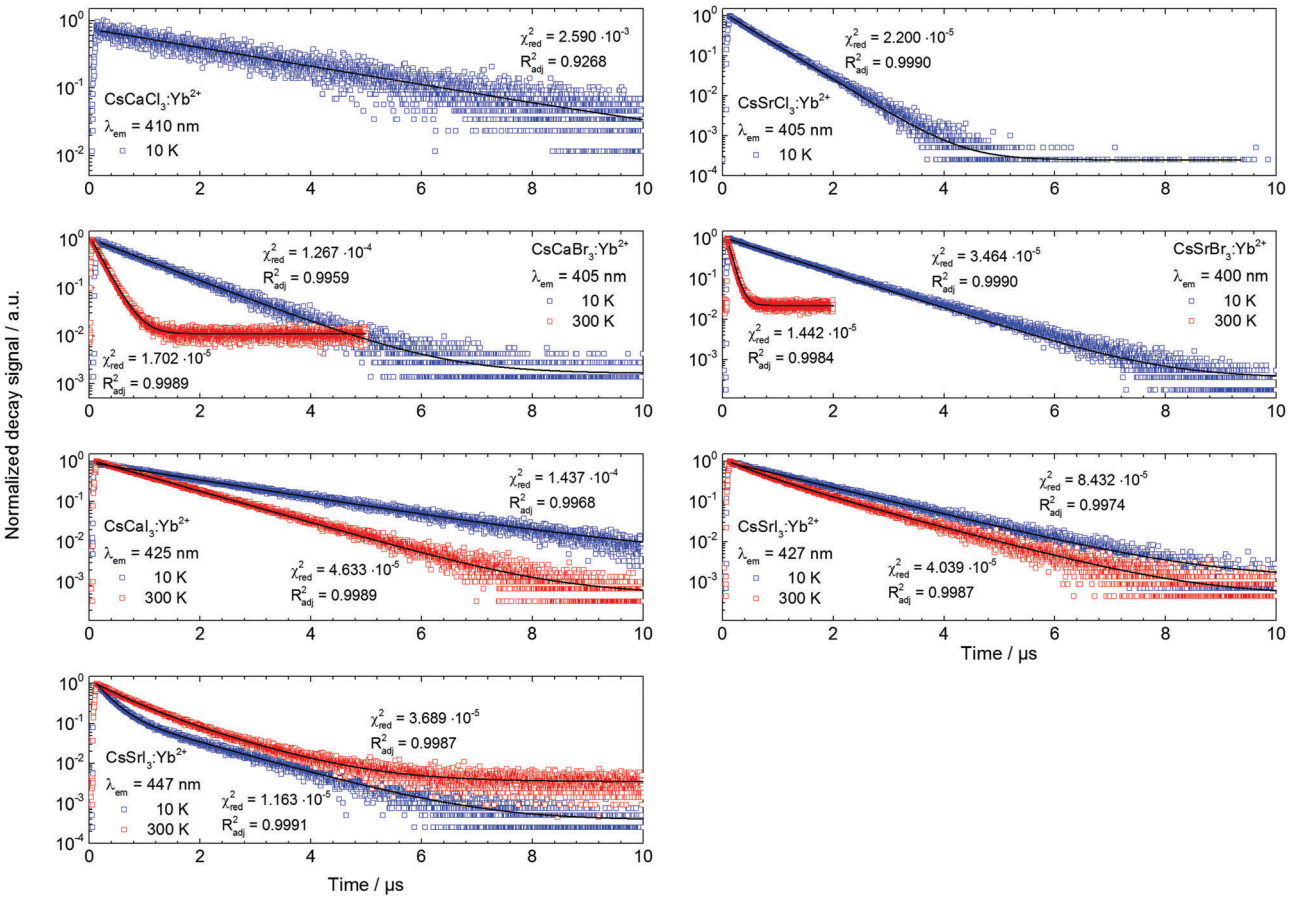


Fig. 2 Semi-logarithmic plots of the luminescence decay of the spin-allowed transition $4f^{13}(^2F_{7/2})5d^1(LS) \rightarrow 4f^{14}(^1S_0)$ of $Yb^{2+}$ doped in $CsCaX_3$ and $CsSrX_3$ (X = Cl, Br, I) at 10 K (blue points) and 300 K (red points). All decay curves were obtained upon excitation at 375 nm. The detected emission wavelengths are given in the graphs for $CsSrI_3:Yb^{2+}$ and two emission bands located at 427 nm and 447 nm are observed. Black lines indicate least-squares fits to single exponential decays or bi-exponential decays in the case of $CsSrI_3:Yb^{2+}$. Statistical figures of merit are given in each case and for the fitting results, see Table 2.

Table 2 Decay times of the excited LS state of $Yb^{2+}$ in $CsCaX_3$ and $CsSrX_3$ (X = Cl, Br, I) at 10 K and room temperature. All decay signals were excited at 375 nm, whereas the corresponding emission wavelengths are depicted in Fig. 2. Errors of the decay times are in the range of $10^{-3}$ µs and hence, disregarded here

| | $\tau_{LS}$/µs | |
|---|---|---|
| Compound | 10 K | 300 K |
| $CsCaCl_3:Yb^{2+}$ | 3.07 | — |
| $CsSrCl_3:Yb^{2+}$ | 0.51 | — |
| $CsCaBr_3:Yb^{2+}$ | 1.00 | 0.21 |
| $CsSrBr_3:Yb^{2+}$ | 0.98 | 0.09 |
| $CsCaI_3:Yb^{2+}$ | 1.98 | 1.12 |
| $CsSrI_3:Yb^{2+}$* | 1.27 ($\lambda_{em}$ = 427 nm) | 0.50, 1.19 |
| | 0.25, 1.13 ($\lambda_{em}$ = 447 nm) | 0.50, 1.07 |

due to the very low doping concentration of 0.1 mol%. Interestingly, the decay time of the spin-enabled transition in $CsCaCl_3:Yb^{2+}$ is extraordinarily long at 10 K compared to the other $Yb^{2+}$-activated halides, which is surprising if the efficient thermal population of the HS state in the chlorides is taken into account.[26] This indicates that the non-radiative rate that characterizes the vibrational relaxation into the HS state has a very strong temperature dependence and becomes almost negligible at 10 K, but rapidly increases at higher temperatures as no spin-enabled emission is observed anymore at room temperature. Contrarily, the corresponding decay time in $CsSrCl_3:Yb^{2+}$ is much shorter at 10 K, which we primarily assign to a symmetry effect as the point symmetry of the $Sr^{2+}$ sites in this compound is actually $C_{4v}$ that may decrease the decay time compared to a higher symmetric environment.[37] Moreover, the size mismatch between $Yb^{2+}$ and $Sr^{2+}$ may also play an important role for the chloride hosts, while its influence is negligible for the bromides. For $CsCaBr_3:Yb^{2+}$, a shorter decay time is observed for the spin-allowed transition at 10 K than for the corresponding iodide. The value of 1 µs agrees well in the order of magnitude with the calculated radiative lifetime of 0.40 µs for the spin-enabled transition in $CsCaBr_3:Yb^{2+}$.[19] In general, more data and calculations for the spin-enabled transition probabilities will provide a more detailed insight to fully understand the impact of different factors that affect the corresponding decay times. The decay times seem to be dependent upon a delicate interplay of symmetry and also non-radiative relaxation pathways into both the excited HS and ground states.

 

Due to the trigonal distortion present in $CsSrI_3:Yb^{2+}$, two spin-allowed emissions are observed for this compound.[25] The higher energetic one (denoted as LS1 emission, $^{(1)}E_u \rightarrow {}^1A_{1g}$ transition according to Fig. 3) shows a single exponential decay curve with a decay time of 1.27 μs at 10 K. The lower energetic spin-allowed emission (denoted as LS2 emission, $^{(1)}A_{2u} \rightarrow {}^1A_{1g}$ transition according to Fig. 3), however, is characterized by a biexponential decay with a short component (0.25 μs) and a long component (1.13 μs). The similarity between the long decay component of the LS2 transition and the decay time of the higher energetic LS state (1.27 μs) is also reflected in a spectral overlap between both respective emission transitions even at 10 K.[25,26] Therefore, the long component is assigned to a decay from the higher energetic LS state, whereas the short component characterizes the transition from the lowest excited LS state giving rise to the LS2 emission at 447 nm (22 370 $cm^{-1}$). According to group theory, the $^{(1)}T_{1u}$-symmetric LS state in $O_h$ symmetry should split up into $^{(1)}E_u$ and $^{(1)}A_{2u}$ states in $D_{3d}$ symmetry. Transitions from both states remain symmetry-allowed in this point group according to the selection rules. The anticipated designation of the different LS states as depicted in Fig. 3 stems from angular overlap model (AOM) considerations as discussed by us earlier.[25,32] Clear experimental evidence for this energetic order may be obtained from the polarized luminescence spectra of $Yb^{2+}$-doped single crystals of $CsSrI_3$.

**3.2.2 Room temperature decay times.** The decay times of the spin-enabled $4f^{13}5d^1 \rightarrow 4f^{14}$ transition of $Yb^{2+}$ in the presented halides shorten at room temperature, which is a manifestation of increasing vibrational relaxation predominantly into the excited HS state. Thermal quenching of the spin-allowed emission of $Yb^{2+}$ in both chlorides $CsCaCl_3$ and $CsSrCl_3$ at higher temperatures than 120 K did not allow the determination of the decay times of the excited LS state at room temperature. For the $Yb^{2+}$-activated bromides, the decay times of the spin-enabled transitions are shorter at room temperature than for the corresponding iodides, which is related to the higher effective vibrational energy of the $[YbBr_6]^{4-}$ moieties that enhances the non-radiative relaxation rate. This is in agreement with the temperature-dependent behaviour of the intensities of the spin-forbidden and spin-enabled emissions of $Yb^{2+}$ in these compounds and is analogous to the trend found for the decay times of the corresponding spin-forbidden 5d–4f transitions of $Yb^{2+}$.[26] The higher vibrational energies promote a faster thermally activated LS to HS relaxation.

A counteracting effect is the size of the exchange splitting $\Delta E_{exch}$ between the excited LS and HS states, which was reported to decrease with higher degree of covalence in the case of $Tb^{3+}$. A smaller HS–LS splitting in the less covalent chlorides could therefore lead to a decrease in decay time from the chlorides to iodides at room temperature.[38,39] The observation of the opposite trend clearly indicates the dominance of the impact of the effective vibrational energies of the $[YbX_6]^{4-}$ moieties and that the exchange splitting does not change significantly upon variation of the anion. This is in very good agreement with our results obtained from the photoluminescence spectra.[25]

Remarkably, the decay times of both spin-allowed emissions in $CsSrI_3:Yb^{2+}$ are only slightly affected by temperature within the considered range. For the higher energetic LS1 emission at 427 nm (23 420 $cm^{-1}$),[25] the single exponential decay curve at 10 K evolves into a biexponential signal with a short component of 0.50 μs at room temperature. Due to the fact that a statistically non-significantly different component is also observed for the lower energetic LS2 emission at 447 nm (22 370 $cm^{-1}$), we assign the short component to the lower excited LS state. By this argument, it is also reasonable that the contribution of the short decay component increases from 10 K to 300 K as the lower excited LS state $^{(3)}A_{2u}$ is non-radiatively populated upon excitation into the higher $^{(3)}E_u$ state. The long decay time component characterizing the $^{(3)}E_u$ state only slightly decreases, which indicates that the non-radiative relaxation rate into the HS states and ground state is very small even at room temperature. This is in agreement with the results obtained from the temperature-dependent emission spectra.[26] An overview of the different radiative and non-radiative pathways in $CsSrI_3:Yb^{2+}$ is depicted in Fig. 3.

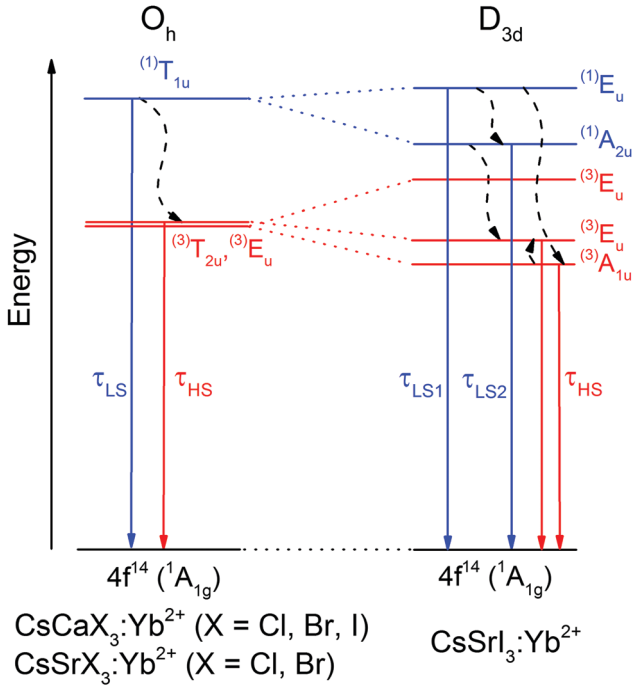


Fig. 3 Simplified energy level scheme of $Yb^{2+}$ in an approximately octahedral coordination in $CsCaX_3$ (X = Cl, Br, I) and $CsSrX_3$ (X = Cl, Br) as well as a trigonally distorted coordination in $CsSrI_3$. Blue lines indicate spin-enabled transitions from excited LS states and red lines denote spin-forbidden transitions from excited HS states. Black dashed arrows indicate non-radiative relaxations and thermal population.

## 4 Conclusions

In this paper, the decay times of the spin-forbidden and spin-enabled transitions of $Yb^{2+}$ doped into the halidoperovskites $CsMX_3$ (M = Ca, Sr; X = Cl, Br, I) were presented for the first time. The spin-forbidden transitions are characterized by decay times in the ms range, similar to decay times observed for $Yb^{2+}$ ions doped into other inorganic compounds. Much shorter

decay times in the range of μs are found for the spin-enabled transitions, which have so far been only sparingly observed. Several trends are observed in the decay times of $Yb^{2+}$ within the different halide hosts that can be related to the local site symmetry and the Yb–ligand distance for the decay times at 10 K. At room temperature, a clear correlation with the strength of the vibrational interaction and vibrational energies is reflected in the decay times for both the spin-enabled and spin-forbidden transitions, which results from the decreasing mode energies of the $[YbX_6]^{4-}$ (X = Cl, Br, I) moieties within the different solids with increasing mass of the halide anion. The exchange splitting between the LS and the HS states does not seem to vary significantly upon variation of the anion and hence, the covalence. In $CsSrI_3$:$Yb^{2+}$, the trigonal distortion of the $Sr^{2+}$ sites complicates the electronic structure of the $Yb^{2+}$ ion in the excited state and the crystal splitting affects the observed decay times. In general, a systematic study of the HS and LS state lifetimes of $Yb^{2+}$ is presented for the first time. This contributes to a better understanding of the impact of the crystal structure of the host material on the decay times of $Yb^{2+}$, which may be valuable for future applications of this activator in scintillators or lighting materials.

## Notes and references

1 P. Dorenbos, *J. Lumin.*, 2003, **104**, 239.
2 H. Terraschke and C. Wickleder, *Chem. Rev.*, 2015, **115**, 11352.
3 P. Dorenbos, *J. Phys.: Condens. Matter*, 2003, **15**, 575.
4 T. S. Piper, J. P. Brown and D. S. McClure, *J. Chem. Phys.*, 1967, **46**, 1353.
5 Z. Pan, C. Duan and P. A. Tanner, *Phys. Rev. B: Condens. Matter Mater. Phys.*, 2008, **77**, 085114.
6 G. Sánchez-Sanz, L. Seijo and Z. Barandiáran, *J. Chem. Phys.*, 2009, **131**, 024505.
7 T. Tsuboi, H. Witzke and D. S. McClure, *J. Lumin.*, 1981, **24/25**, 305.
8 T. Tsuboi, D. S. McClure and W. C. Wong, *Phys. Rev. B: Condens. Matter Mater. Phys.*, 1993, **48**, 62.
9 S. W. Bland and M. J. A. Smith, *J. Phys. C: Solid State Phys.*, 1985, **18**, 1525.
10 E. Loh, *Phys. Rev.*, 1969, **184**, 348.
11 G. Blasse, G. J. Dirksen and A. Meijerink, *Chem. Phys. Lett.*, 1990, **167**, 41.
12 V. P. Dotsenko, I. V. Berezovskaya, P. V. Pyrogenko, N. P. Efryushina, P. A. Rodnyi, C. W. E. v. Eijk and A. V. Sidorenko, *J. Solid State Chem.*, 2002, **166**, 271.
13 S. Lizzo, E. P. K. Nagelvoort, R. Erens, A. Meijerink and G. Blasse, *J. Phys. Chem. Solids*, 1997, **58**, 963.
14 S. Lizzo, A. Meijerink and G. Blasse, *J. Lumin.*, 1994, **59**, 185.
15 A. B. Parmentier, J. J. Joos, P. F. Smet and D. Poelman, *J. Lumin.*, 2014, **154**, 445.
16 V. Bachmann, T. Jüstel, A. Meijerink, C. Ronda and P. J. Schmidt, *J. Lumin.*, 2006, **121**, 441.
17 Z. Zhang, O. M. ten Kate, A. C. A. Delsing, M. J. H. Stevens, J. Zhao, P. H. L. Notten, P. Dorenbos and H. T. Hintzen, *J. Mater. Chem.*, 2012, **22**, 23871.
18 C.-K. Duan and P. A. Tanner, *J. Phys.: Condens. Matter*, 2008, **20**, 215228.
19 G. Sánchez-Sanz, L. Seijo and Z. Barandiáran, *J. Phys. Chem. A*, 2009, **113**, 12591.
20 G. Sánchez-Sanz, L. Seijo and Z. Barandiáran, *J. Chem. Phys.*, 2010, **133**, 114506.
21 G. Sánchez-Sanz, L. Seijo and Z. Barandiáran, *J. Chem. Phys.*, 2010, **133**, 114509.
22 A. J. Salkeld, M. F. Reid, J.-P. R. Wells, G. Sánchez-Sanz, L. Seijo and Z. Barandiarán, *J. Phys.: Condens. Matter*, 2013, **25**, 415504.
23 H. Ramanantoanina, F. Cimpoesu, C. Göttel, M. Sahnoun, B. Herden, M. Suta, C. Wickleder, W. Urland and C. Daul, *Inorg. Chem.*, 2015, **54**, 8319.
24 C. Bulloni, A. García-Fuente, W. Urland and C. Daul, *Phys. Chem. Chem. Phys.*, 2015, **17**, 24925.
25 M. Suta, W. Urland, C. Daul and C. Wickleder, *Phys. Chem. Chem. Phys.*, 2016, **18**, 13196.
26 M. Suta and C. Wickleder, *Adv. Funct. Mater.*, 2017, **27**, 1602783.
27 S. Lizzo, A. Meijerink, G. J. Dirksen and G. Blasse, *J. Lumin.*, 1995, **63**, 223.
28 B. Moine, B. Courtois and C. Pedrini, *J. Lumin.*, 1991, **48 & 49**, 501.
29 S. Lizzo, A. Meijerink, G. J. Dirksen and G. Blasse, *J. Phys. Chem. Solids*, 1995, **56**, 959.
30 W. J. Schipper and G. Blasse, *J. Solid State Chem.*, 1991, **94**, 418.
31 M. S. Alekhin, D. A. Biner, K. W. Krämer and P. Dorenbos, *Opt. Mater.*, 2014, **37**, 382.
32 M. Suta and C. Wickleder, *J. Mater. Chem. C*, 2015, **3**, 5233.
33 E. Rowe, P. Bhattacharya, E. Tupitsyn, M. Groza, A. Burger, N. J. Cherepy, S. A. Payne, B. W. Sturm and C. Pédrini, *IEEE Trans. Nucl. Sci.*, 2013, **60**, 1057.
34 R. D. Shannon, *Acta Crystallogr., Sect. A: Cryst. Phys., Diffr., Theor. Gen. Crystallogr.*, 1976, **32**, 751.
35 G. Schilling and G. Meyer, *Z. Anorg. Allg. Chem.*, 1996, **622**, 759.
36 P. Fontana, J. Schefer and D. Pettit, *J. Cryst. Growth*, 2011, **324**, 207.
37 H. F. McMurdie, J. d. Groot, M. Morris and H. E. Swanson, *J. Res. NBS*, 1969, **73A**, 621.
38 P. Dorenbos, *J. Phys.: Condens. Matter*, 2003, **15**, 6249.
39 J. Shi and S. Zhang, *J. Phys.: Condens. Matter*, 2003, **15**, 4101.

 